J Mater Sci (2010) 45:1579–1587
DOI 10.1007/s10853-009-4127-y

The enhancement of creep in Al–22 wt% Ag alloy by cyclic stressing

M. A. Mahmoud · A. F. Abd El-Rehim

Received: 10 October 2009 / Accepted: 10 December 2009 / Published online: 29 December 2009

Abstract The plastic deformation behavior of Al–22 wt% Ag alloy during phase transformation was investigated by studying the creep behavior under cyclic stress reduction of low frequencies. The cyclic creep curves obtained describe clearly the cyclic stress acceleration behavior. Increasing frequency of cyclic stress reduction enhanced the creep deformation depending upon the combination of the experimental variables as testing temperature, aging temperature and static creep rate. The irregularity in the creep parameters, n, β and ε_{st} with increasing aging temperatures, has been explained on the basis of structure transformations occurring in Al–Ag system and their mode of interaction with mobile dislocations.

Introduction

Al–Ag based alloys are often used in technological applications because of their casting and workable properties [1]. Also, the system serves as a useful model for better understanding the kinetics of the precipitation and coarsening of plate-shape precipitates [2]. The basic sequence of decomposition in a supersaturated solid solution of Al–Ag system is known to be spherical G.P. zones (tetrahedral) → metastable γ'-phase → equilibrium γ-phase (hcp) [3]. Dubey et al. [4], using small angle X-rays scattering (SAXS) studies, concluded that the composition of G.P. zones ($\sim Ag_2Al$) remains constant over a wide temperature range from 20 to 250 °C. Previous studies [5, 6] on Al–Ag system obtained the experimental evidence for the formation of an ordered η-state of G.P. zones below 170 °C and a disordered ε-state above this temperature. Positron trapping method showed that the coarsening of G.P. zones takes place simultaneously with the formation and growth of γ'-precipitates during isothermal aging above 473 K [4, 7]. The critical temperature for the cessation of the dislocation splitting mechanism in Al–15 wt% Ag alloy was found [8] to be 375 ± 5 °C; consequently, the transformation from γ'-phase to the equilibrium γ-phase occurs above $\sim$375 °C.

Under service conditions, many structural members are subjected to combinations of static and cyclic stresses. The development of materials and the subsequent design of the components for such applications is of great importance. Continued creep at constant stress results from simultaneous work hardening and recovery processes is relatively well understood. While most of the creep literature deals with the determination of creep parameters under constant stress, there are comparatively few investigations on the effect of stress changes. The cyclic creep behavior relative to the static creep behavior can vary considerably both qualitatively and quantitatively. Stress cycling during creep can cause either cyclic softening or cycling hardening. When cyclic softening is the predominant effect of stress cycling, the resulting cyclic behavior is the cyclic stress acceleration. On the other hand, under certain conditions, cyclic hardening is caused by stress cycling, and then the cyclic creep behavior is cyclic stress retardation. The cycling hardening phenomenon is predominant in single crystals and at low stresses and low temperatures. Cyclic creep acceleration has been observed in aluminum [9, 10], copper [9, 11], lead [11, 12] and Al–Zn alloys [13]. Cyclic creep retardation has been reported for Cd [9], Zn [14], Ni alloys [15], and Cu alloys [16]. Recently, cyclic creep acceleration has been observed in Al–Cu alloys [17], Al–Zn

M. A. Mahmoud (✉) · A. F. Abd El-Rehim
Physics Department, Faculty of Education, Ain Shams University, P.O. Box 5101, Heliopolis, Roxy, 11771 Cairo, Egypt
e-mail: moustafa_a_mahmoud@hotmail.com

alloy [18], and Al–Mg alloy [19]. Cases of acceleration and retardation of creep for the same metal have been reported [10] for an aluminium alloy and pure aluminium.

In the course of a previous study by the authors [20, 21] on the effect of amplitude of cyclic stress reduction and the effect of the torsional oscillations of different amplitudes on the creep of Al–Ag alloys, an acceleration of both transient and steady state creep rates has been noticed. Since cyclic creep rates are reported as strain time, it is important to ask whether or not the cyclic creep rate is frequency dependent. However, a systematic study of the effect of low frequency of cyclic stress reduction on the creep behavior of Al–Ag regime has not been studied. The present investigation is an attempt to characterize the features of repeated cyclic stress reduction of different low frequencies (cyclic creep) on Al–22 wt% Ag in contrast to the static stress deformation (static creep).

Experimental techniques

The material investigated, Al–22 wt% Ag alloy, was prepared by melting pure aluminum and silver (99.999%) under vacuum in a high-purity graphite crucible. After solidification, the ingot was homogenized at 823 K for 4 days and then swaged in the form of wires of 0.35 mm in diameter and length 0.05 m for creep study. To make the tested specimens have the same thermal history, all wires were annealed for 3 h at 798 K to cancel the cold work introduced during swaging and were then quenched in iced water. Immediately after quenching, the specimens were aged for 1 h at different aging temperatures ($T_a = 423$, 453, 493, 563, 613 and 683 K) to produce the microstructures required of G.P. zones, metastable γ'-phase, equilibrium γ-phase.

A constant load static creep machine was modified so that cyclic and/or static creep experiments without completely unloading can be carried out using the machine. Such modifications done are described in detail elsewhere [22].

The creep tests have been performed under cyclic stress corresponding to a static stress of $\sigma_{max} = 68$ MPa (maximum or peak stress) lowered through unloading by constant amplitude of cyclic stress reduction $\sigma_{cy} = 23.8$ MPa at different testing temperatures, T_t, of 348, 368, 388 and 408 K with the working wire in a vertical position. Such cyclic stress reduction with partial unloading—time-dependent stress—has the form of a sinusoidal wave (see Fig. 1) with frequency in the range 0.2–0.44 Hz. The aging and testing temperatures were monitored with chromel-alumel thermocouples held in contact with the test specimen and were maintained to within ±1 K. Transmission electron microscopy (TEM) micrographs investigated by the author for the same alloy show the existence of fine G.P. zones, coarse G.P. zones, reversion of G.P. zones into metastable γ'-phase, coarse metastable γ'-phase and the equilibrium γ-phase were published elsewhere [23, 24].

Experimental results

The cyclic softening that leads to cyclic creep acceleration occurs only above a threshold stress [20]; accordingly, the amplitude of cyclic stress reduction used ($\sigma_{cy} = 23.8$ MPa) exceeds the threshold stress for the alloy understudy. The stress was cycled between peak stress of 68 MPa and minimum stress, $\sigma_{min} = 44.2$ MPa, i.e. the amplitude of cyclic stress reduction, $\sigma_{cy} = 23.8$ MPa (see Fig. 1). The specimens of Al–22 wt% Ag alloy pre-aged at different aging temperatures ($T_a = 423$–683 K) for 1 h were crept under different testing temperatures ($T_t = 348$–408 K) until the steady state stage was attained. Figure 2 demonstrates representative curves of strain–time relations for specimens pre-aged at 423 and 683 K worked at testing temperature of 348 K with imposed cyclic stress reduction of different frequencies, $\nu = 0.2$, 0.28, 0.36 and 0.44 Hz. The relation for samples not subjected to cyclic stress reduction (static creep) is also drawn on identical scales for comparison. All the strain–time relations of Fig. 2 showed the same normal

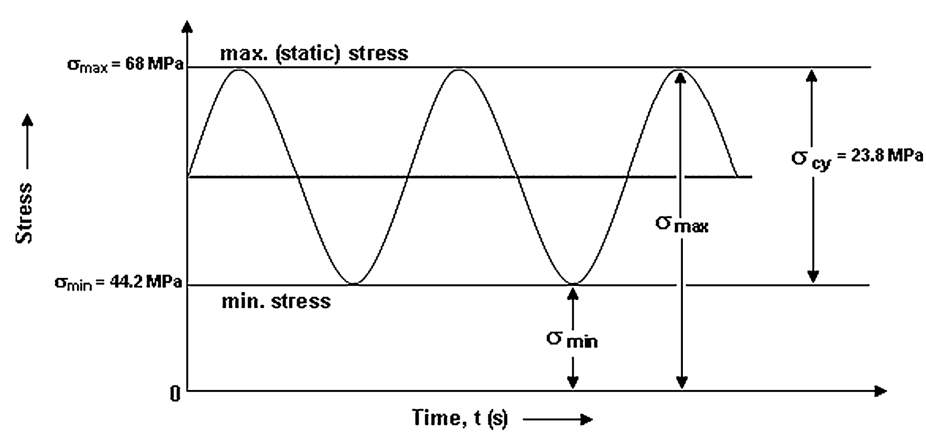

Fig. 1 Stress–time variation for fluctuating stress

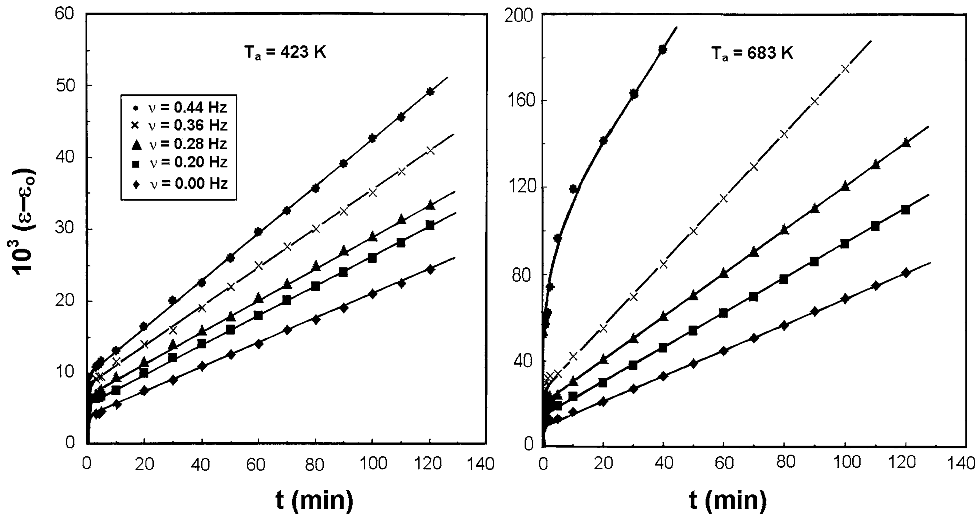

Fig. 2 Representative strain–time curves for representative specimens of Al–22 wt% Ag alloy crept under cyclic stress reduction, $\sigma_c = 23.8$ MPa of different frequencies, ν, at testing temperature of 348 K. The applied frequencies and aging temperatures, T_a, are indicated

creep behavior under the different conditions investigated. A monotonic shift toward higher strains and creep rates is observed with increasing the applied frequency compared to static stress of similar maximum or peak stress. The most interesting observation of the experimental results is the drastic difference between the static creep behavior and cyclic creep behavior. The results reported here are in contrast to that obtained by Lorenzo and Laird [10] on their work on polycrystalline copper where no frequency effect was detected. In the present work, the transient stage is characterized by a short duration time (~3–5 min) while a steady state stage lasts 3 h with a constant creep rate without specimens failure except specimens aged at 683 K and worked at maximum frequency ($\nu = 0.44$ Hz) and maximum testing temperature ($T_t = 408$ K).

The transient creep strain, ε_{tr}, was found to obey a relation in the form [25]:

$$\varepsilon_{tr} = \beta(t_{tr})^n \quad (1)$$

where t_{tr} is the transient creep time (in s), β and n are constants depending on the test conditions. From the relations between ln ε_{tr} and ln t at different aging and testing temperatures for different magnitudes of frequency, ν, the parameter n is obtained as the slope of the straight lines. The transient creep parameter β was deduced from the intercept at ln ε_{tr} axis. The aging temperature, T_a, dependence of the parameter n at different values of testing temperatures for different magnitudes of ν is given in Fig. 3, and Fig. 4 shows the same relations for the parameter β. The steady state creep rate, ε_{st}, values of the

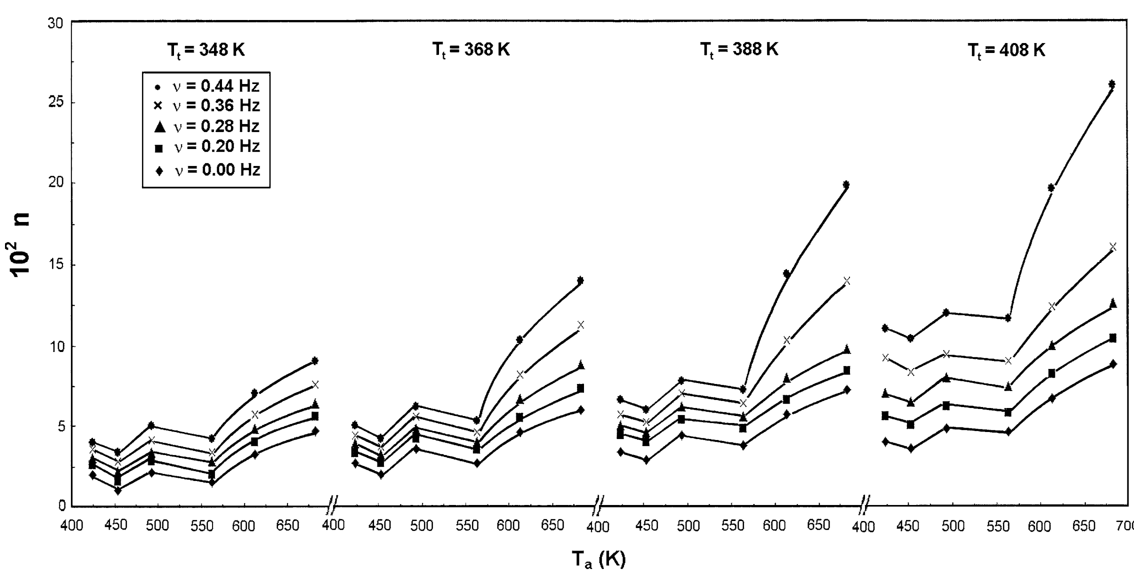

Fig. 3 Dependence of transient creep exponent n on aging temperature T_a at different frequencies, ν, of cyclic stress reduction. Testing temperatures, T_t, and the frequency applied are indicated

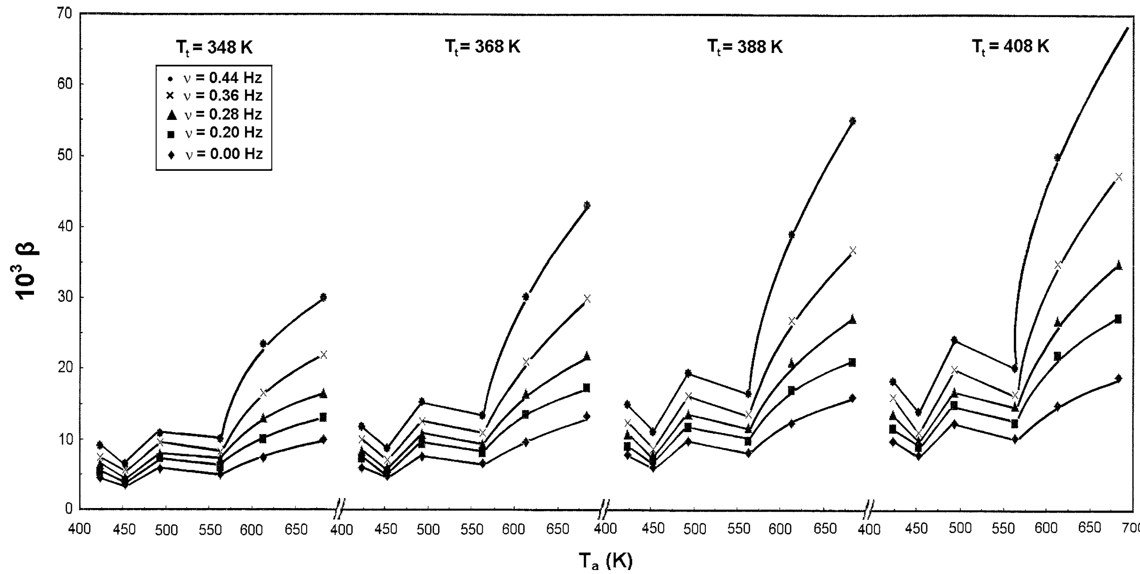

Fig. 4 Dependence of transient creep exponent β on aging temperature T_a at different frequencies, v, of cyclic stress reduction. Testing temperatures, T_t, and the frequency applied are indicated

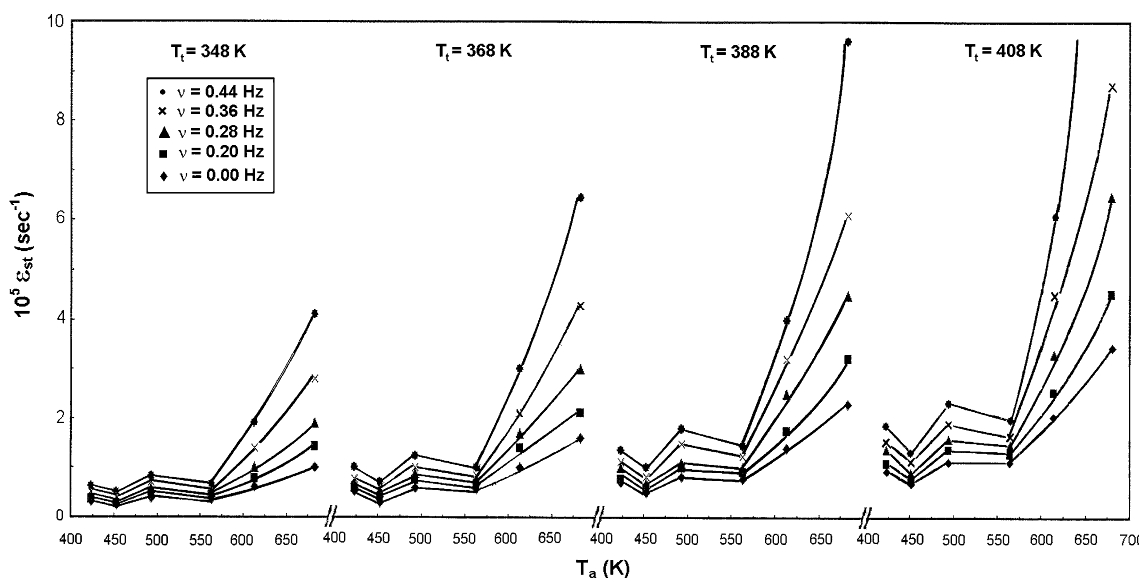

Fig. 5 Aging temperature dependence of the creep parameter, ε_{st}, on T_a at different frequencies, v, of cyclic stress reduction. Testing temperatures, T_t, and the frequency applied are indicated

tested samples are calculated from the slopes of the linear parts of the creep curves of Fig. 2. Figure 5 demonstrates these values as a function of different aging temperatures at different testing temperatures and frequencies superimposed.

It is important to point out that:

(i) The general thermally induced behavior ε_{st} in Fig. 5 is similar to that of n and β (Figs. 3 and 4).

(ii) For a given aging temperature and frequency, the value of n, β and ε_{st} tends to increase as testing temperatures increase.

(iii) The peak value of n, β and ε_{st} at $T_a = 423$ and 493 K shows sudden drop at $T_a = 453$ and 563 K followed by further increase at higher aging temperatures, $T_a = 613$ and 683 K.

(iv) The drop values of n, β and ε_{st} induced at $T_a = 453$ K are always more deep than those at $T_a = 563$ K, and the following rise in these values is more high at $T_a = 613$ K than that at $T_a = 493$ K.

The influence of different frequencies superimposed on the levels of n, β and ε_{st} for specimens aged at different aging temperatures is demonstrated in Figs. 6, 7, and 8

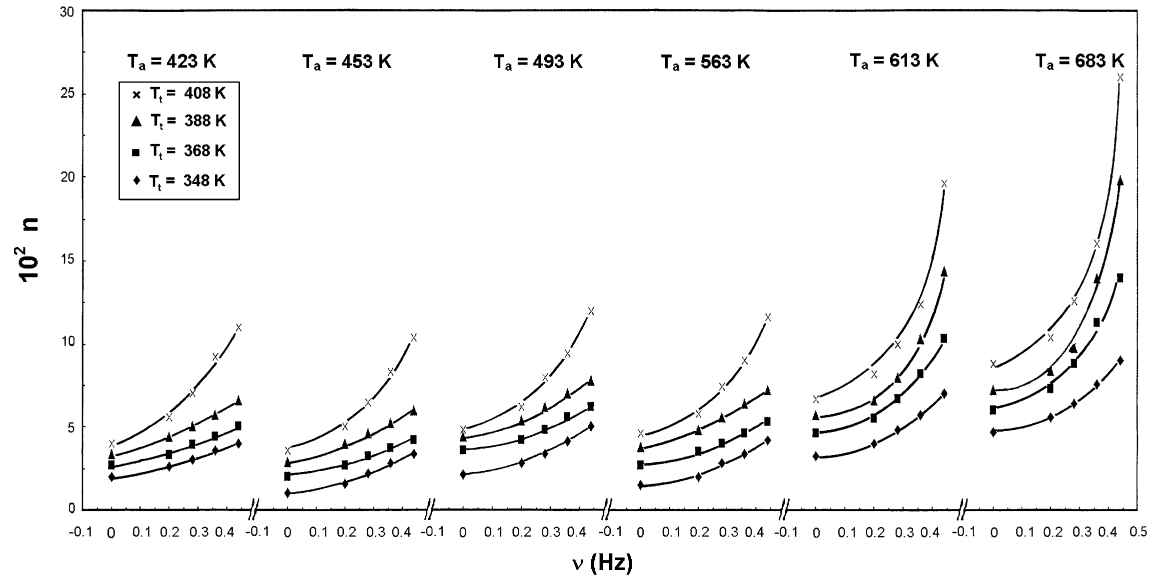

Fig. 6 Dependence of transient creep *n*, on frequency of the cyclic stress reduction. Testing temperatures, T_t, and the frequency applied are indicated

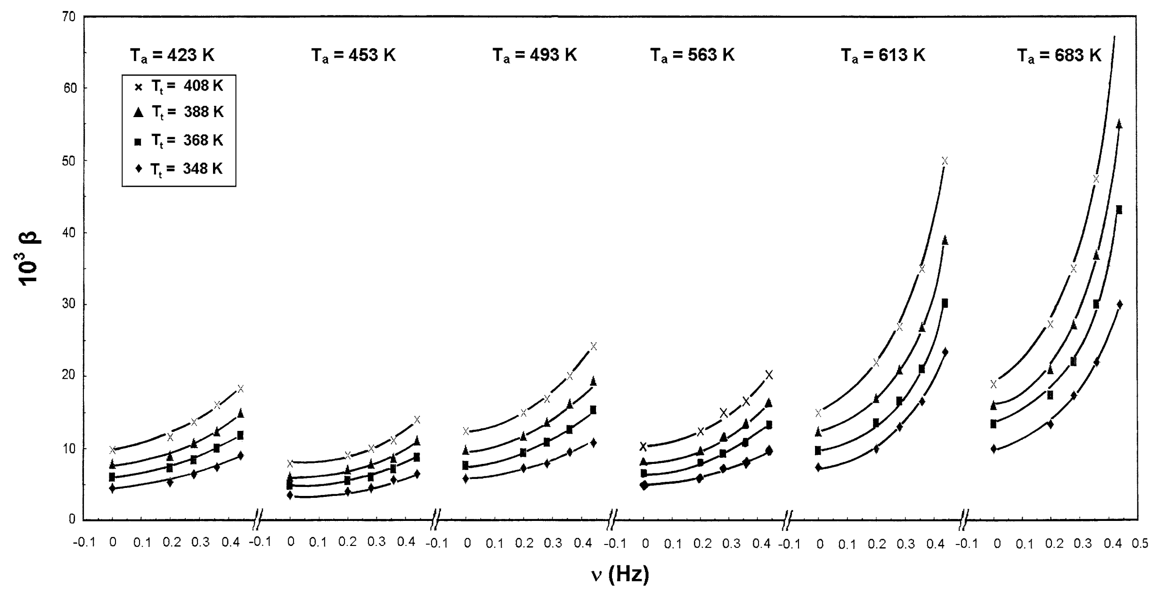

Fig. 7 Dependence of transient creep parameter *β* on frequency of the cyclic stress reduction. Testing temperatures, T_t, and the frequency applied are indicated

respectively. These figures indicate that the magnitudes of n, β and ε_{st} increase with the increase in frequency values affecting the testing specimens.

Discussion

The irregularity in the values of n, β and ε_{st} with the increase in the aging temperature as shown in Figs. 3, 4, and 5 can be explained on the basis of structural changes generated in Al–Ag system; spherical G.P. zones → metastable γ'-phase → equilibrium γ-phase and their interaction with moving dislocations [26, 27]. In the present study, quenching the specimens from 423 K results in the formation of intense fine ordered η-state of G.P. zones and a disordered ε-state zones above this temperature up to 453 K [5, 28]. These fine precipitates are considered as second phase particles, whereas they act as obstacles or pinners for moving dislocations enhancing the creep resistance in specimens investigated [1, 3, 21, 23, 27, 29].

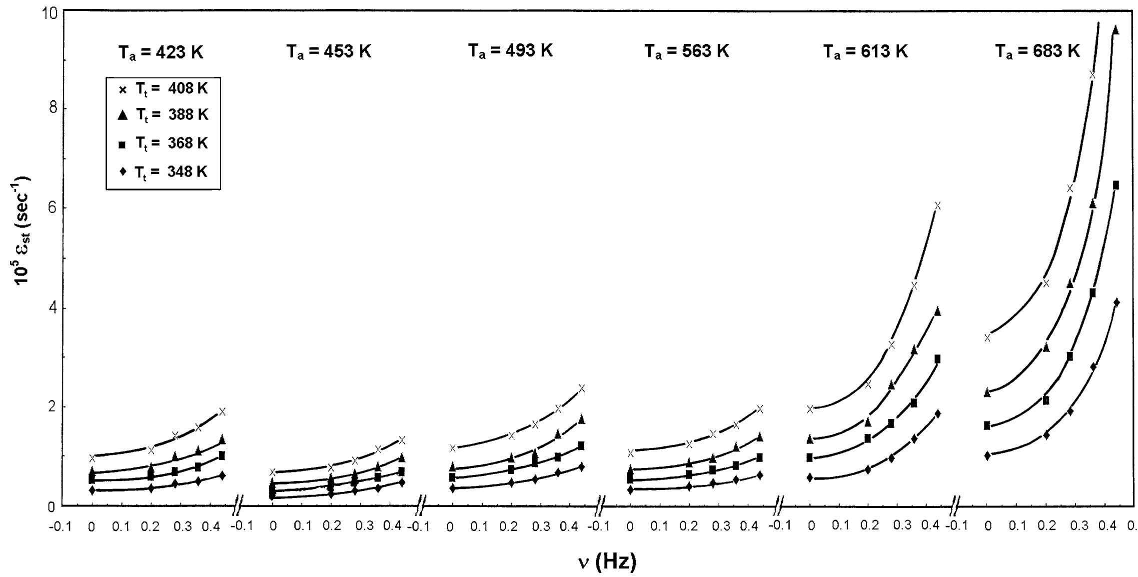

Fig. 8 Dependence of the creep parameter, ε_{st}, on frequency of the cyclic stress reduction. Testing temperatures, T_t, and the frequency applied are indicated

The following increase in n, β and ε_{st} was found in the aging temperatures range 453–493 K can be explained due to coalescence and partial dissolution of G.P. zones. G.P. zones of large sizes and less numbers are known to be less competent as barriers for moving dislocations [21, 23, 27, 29, 30]. Aging the specimens at the temperature range 493–563 K yields alloy containing a few number of semi-coherent γ' precipitates that grow at the expense of the more soluble G.P. zones already existing in the matrix [31]. The plate-like γ' precipitates of small size concurrently with the remainder coalescence zones are known [26, 29] to block dislocations motion very effectively, as a result lower values of n, β and ε_{st} are expected. The enhanced creep of n, β and ε_{st} in the temperatures range 563–613 K as observed in Figs. 2, 3, and 4 might be ascribed to the coarsening of semi-coherent γ' precipitates together with early precipitation stages of γ-phase [1, 20, 23]. Such a coarsening results in an increase in precipitates thickness accompanying with a decrease in their numbers. So, the number of barriers for dislocation motion will extensively be reduced and the recovery of dislocations occurs by a higher rate, leading to less of strength [1, 20, 27, 32]. The plainly increase in the creep parameters at the temperatures range 613–683 K is based on the fact that at this temperature range, the matrix gets ready to form the equilibrium γ-plates as the metastable phases (G.P. zones and γ' precipitates) dissolved in the matrix and completely disappeared [24]. The γ-plates are very thick and of less volume fraction, so they are considered to be less efficient as impeding agents for dislocation motion [31, 32].

As shown in Figs. 3, 4, and 5, under the same conditions of testing temperatures and frequencies superimposed, the levels of n, β and ε_{st} for specimens aged at 423 K are smaller than those obtained for specimens aged at 493 K. Also, the levels of n, β and ε_{st} for specimens pre-aged at $T_a = 453$ K are more deep as compared with their level for specimens pre-aged at $T_a = 563$ K. These results are consistent with those obtained before [21] and confirmed that (i) ordered η-state of G.P. zones of small size and large number resist mobile dislocation by a higher rate compared with coarse G.P. zones of less number. (ii) Disordered ε-state zones inhibit the dislocation motion more effectively compared with γ' precipitates of less number and small size.

The most important observation made in the course of the present investigation was that the cyclic creep behavior of Al–22 wt% Ag can vary considerably relative to the static creep behavior. The cyclic creep behavior in polycrystalline and single aluminum were qualitatively similar [10]. Therefore, cyclic softening and hardening are not grain boundary related phenomena. It should be recognized that neither of these cyclic creep behaviors can be predicted from any analysis of static creep data and thus they are uniquely characteristic to cyclic stressing. In the course of cyclic acceleration, the change in the mode of stressing from static to cyclic increases the creep rates. Since the peak stress during cycling is the same as the initial static stress, the increase of creep rates necessarily means softening and can be ascribed to a decrease in the internal stress, σ_i which is associated with smaller work-hardening rate. In a first order approximation, the stress dependence of cyclic creep acceleration behavior obeys the equation:

$$\sigma_M = \sigma_i + \sigma_e \quad (2)$$

where σ_M is the applied stress and σ_e is the effective stress determining the creep rate. Thus, the investigation of the dependence of the creep behavior on σ_M also corresponds to the dependence on σ_i. The stress cycling induces a change in the dislocation obstacles rearrangements, i.e. induces dislocation rearrangements such as to facilitate the dislocation motion by helping it to surmount the precipitates which act as dislocation barriers [24] and produce lower internal stresses and work hardening. So, the softening process results from the transformation of a dislocation structure which is characteristic to the static mode of stressing into a structure characteristic to cyclic stress. It is suggested that the change in the obstacle structure takes place under the influence of internal stress, σ_i rather than the applied stress, σ_M. The experimental results do, however, indicate that this transformation is sensitively depending upon the frequency of the cyclic stress reduction. The results obtained indicate that increasing the frequency of cyclic stress reduction results in a greater strain accumulation associated with small work-hardening rate (see Figs. 5, 6, and 7). This additional softening can best understood in terms of the temporary pinning of mobile dislocation which are gradually freed as magnitude of frequency increases. At the same time, the additional energy introduced by frequency together with stress cycling causes the rearrangements of the dislocation-obstacles structure, enhance the recovery during creep process [33] and reduce the value of σ_i. The testing temperature dependence of the cyclic creep behavior observed in the present study is consistent with the qualitative ideas developed so far. At higher testing temperatures, however, even during static creep dislocation rearrangements take place due to spontaneous thermal recovery. The characteristic dislocation processes that may be involved in the softening phenomena discussed before will be reported in the future.

The activating energy of the transient or the steady state creep, E, was calculated using an Arrhenius equation of the form [34]:

$$\beta = \text{Constant exp.}\left(\frac{E}{KT_t}\right) \quad (3)$$

$$\varepsilon_{st} = \text{Constant exp.}\left(\frac{E}{KT_t}\right) \quad (4)$$

where K is the Boltzmann constant, T_t is the testing temperature in Kelvin. The relation between ln β and $10^3/T_t$ K^{-1} (Fig. 9) and ln ε_{st} versus $10^3/T_t$ K^{-1} (Fig. 10) gave straight lines for different aging temperatures and frequencies. The calculated activation energies were found to be independent on either frequency or aging temperature, but showed dependence on the kind of stage. For transient and steady state creep stages, the calculated energies assumed values ~17 kJ/mol and ~23 kJ/mol, respectively. The close values of these activation energies consist with conclusion that the mechanism responsible for the creep process is the dislocations intersection mechanism [1, 22, 24, 27].

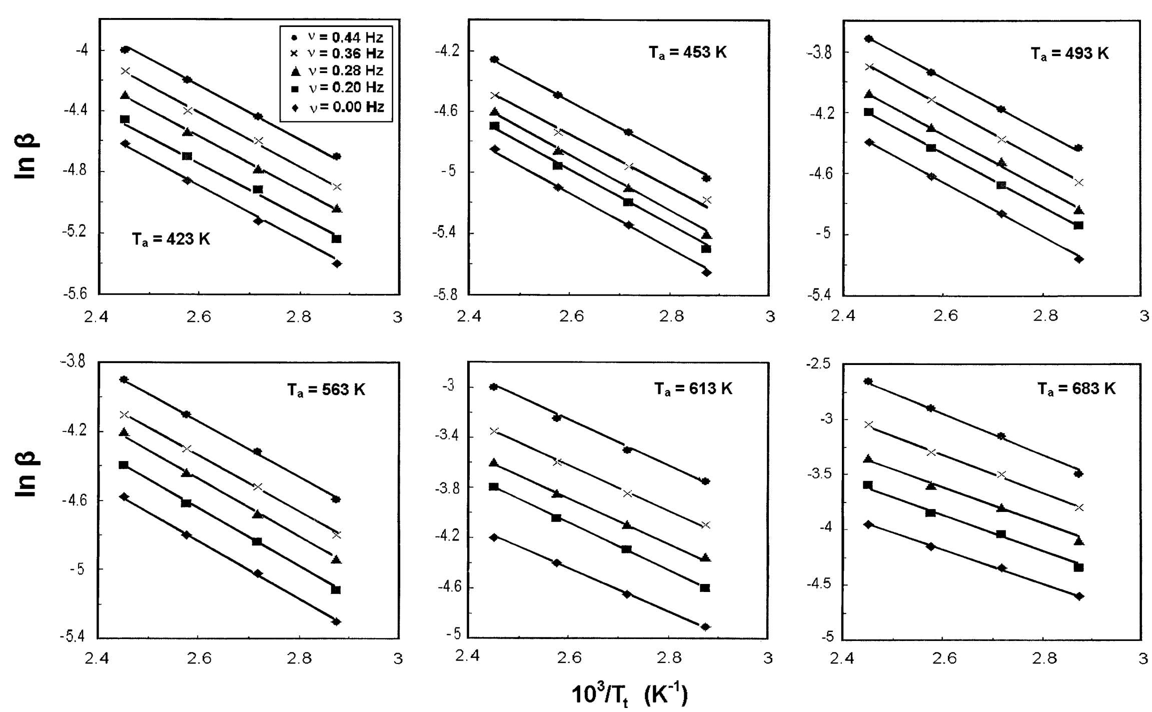

Fig. 9 The relation between ln β and $10^3/T_t$ at different frequencies, ν, and aging temperature, T_a

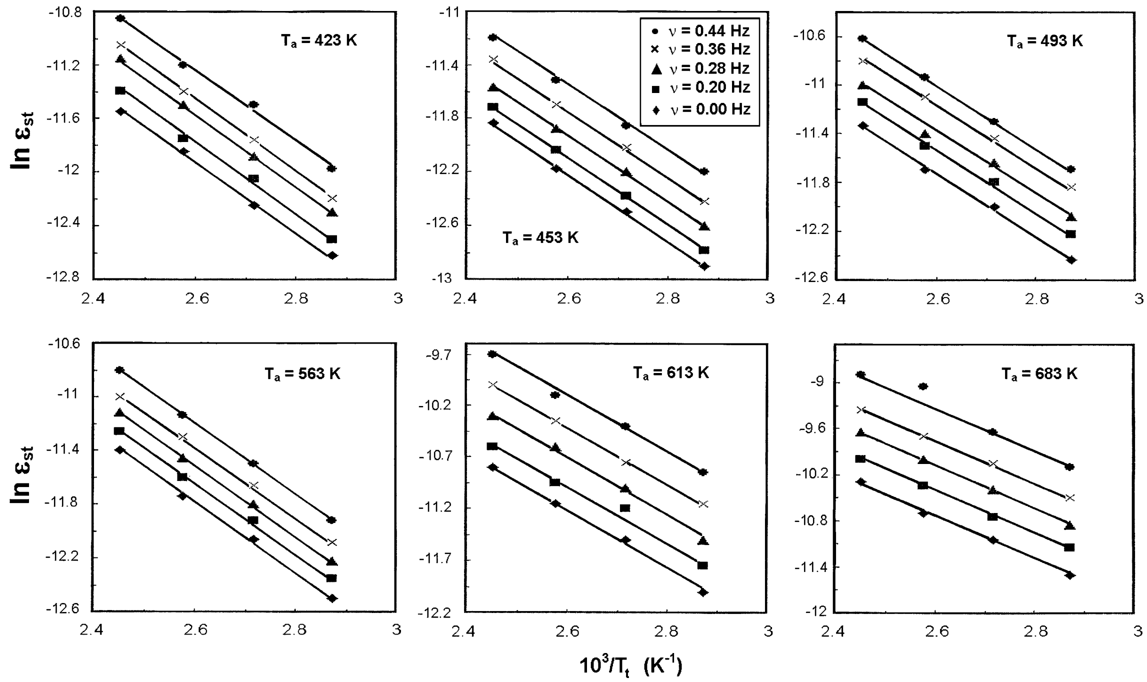

Fig. 10 The relation between ln ε_{st} and $10^3/T_t$ at different frequencies, v, and aging temperature, T_a

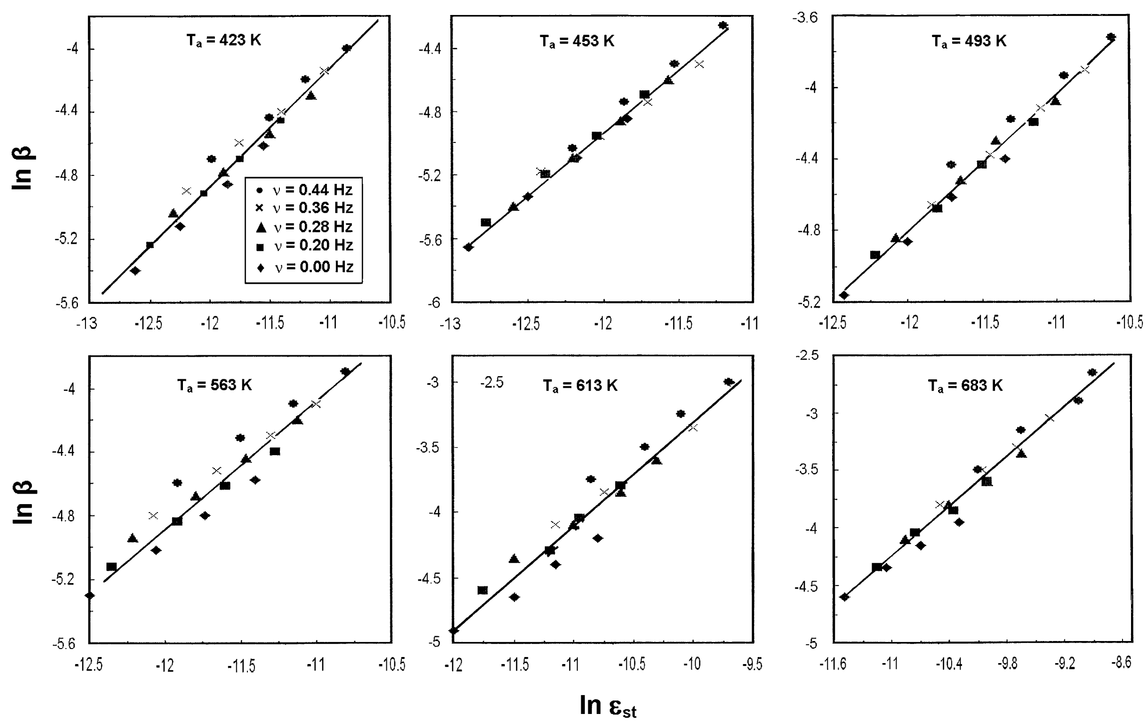

Fig. 11 A plot relating ln β and ln ε_{st} at different frequencies, v, and aging temperature, T_a

As creep is a continuous thermally activated process, the parameter β was reported to correlate with steady state creep rate ε_{st} through the relation [35]:

$$\beta = \beta_0 (\varepsilon_{st})^{\alpha} \quad (5)$$

where β_0 is a constant and $\alpha = (\delta \ln \beta / \delta \ln \varepsilon_{st})$ relates both the transient and the steady state creep stages. α is the slope of the straight lines relating ln β and ln ε_{st} given in Fig. 11 which shows that α is a frequency independent ratio with a mean value of 0.8. These values of α are comparable with those obtained by Abd-El salam et al. [36, 37] in their study on Al–40 wt% Zn. This relatively high value of α confirms that the mechanism controlling the transient stage still act upon the steady stage and may be explained as follows: the middle of primary creep stage is characterized by a nearly constant rate [38], this property is named as sub-steady state creep stage. At the end of sub-steady state stage, the hardening process becomes the predominate process due to the piling up of the moving dislocations on their slip planes resulting in a decrease in their density. Then, the re-distribution of dislocations takes place and a balance between the hardening rate and recovery rate occurs, at which the steady state stage begins to appear.

Conclusions

1. The irregularity in the values of n, β and ε_{st} with the increase in the aging temperature has been explained on the basis of structural changes generated in Al–Ag system and their interaction with moving dislocations.
2. The creep rate in Al–22 wt% Ag increases by cycling the applied stress depending on the combination of the experimental variables.
3. The transformation of the characteristic dislocation obstacle structure during cyclic stress acceleration occurs under the influence of internal stress.
4. The frequency of the stress cycling and testing temperature are effective in enhancing both the transient and steady state creep rates.
5. The calculated activation energies were found to be independent on either frequency or aging temperature, but showed dependence on the kind of stage.
6. The high values of α suggested a high dependence of steady state creep on the transient creep stage.

References

1. Deaf GH, Yossef SB, Mahmoud MA (1996) Phys Stat Sol (a) 158:79
2. Sagoe-Crentsil KK, Brown LC (1990) Philos Mag A 61:451
3. Graiss G, Mahmoud MA (2001) J Mater Sci 36:1507. doi:10.1023/A:1017505031452
4. Dubey PhA, Schonfeld B, Kostorz G (1991) Act Metall 39:1161
5. Dlubeck G, Wendrock G, Pawelzyk K (1993) Phys Stat Sol (a) 140:311
6. Malik A, Schonfeld B, Kostorz G (1997) Z Metallkd 88:625
7. Moore KT, Howe JM (2000) Acta Mater 48:4083
8. Moore KT, Howe JM, Veblen DR (2002) Metall Mater Trans 33A:1561
9. Feltner CE (1963) Tech document rep no RTD-T.D.R., vol 63, p 4169
10. Lorenzo F, Laird C (1984) Acta Metall 32(5):681
11. Melek AH, Evershed AV (1960) J Inst Met 88:411
12. Greenwood JN (1949) Proc ASTM 49:834
13. Blum W, Rosen A, Cegielska A, Martin JI (1989) Acta Metall 37:2439
14. Price AT (1967) J Inst Met 95:87
15. Webster GA, Picaiceyi BJ (1966) Trans Am Soc Met 59:847
16. Davies PW, Wilshire B (1967) Metallurgia 76:93
17. Graiss G, Mahmoud MA, Ashry AH, Abdelkhalekh AM, Abd El-Rehim AF (2004) Phys Stat Sol (a) 201:2295
18. Abd El-Salam F, Abdel-Khalekh AM, Nada RH (2007) Physica B 388:219
19. Abd El-Rehim AF, Mahmoud MA (2009) Mater Sci Technol (in press)
20. Graiss G, Mahmoud MA (2000) Cryst Res Technol 35:95
21. Mahmoud MA, Graiss G (2002) J Mater Sci 37:2215. doi:10.1023/A:1015304913637
22. Abd El-Rehim AF (2004) Ph.D. thesis, Ain Shams University, Cairo, p 68
23. Mahmoud MA (2001) Physica B 304:456
24. Mahmoud MA (2001) Phys Stat Sol (a) 186:143
25. Abd El-Rehim AF (2008) J Mater Sci 43:1444. doi:10.1007/s10853-007-2312-4
26. Ferramate M, Doherty RD (1979) Acta Metall 27:1603
27. Deaf GH, Yossef SB, Mahmoud MA, Graiss G, Kenawy MA (1996) Phys Stat Sol (a) 158:471
28. Nabarro N, Howe JM (1991) Philos Mag A 63:645
29. Graiss G, Mahmoud MA (2000) Fizika A 9:137
30. Kanadani T, Umada A (1995) Phys Stat Sol (a) 148:K23
31. Sagoe-Crentsil KK, Brown LC (1991) Philos Mag A 63:477
32. Rajab KE, Doherty RD (1989) Acta Metall 38:2709
33. Beshai MHN, Deaf GH, Abdel-Khalekh AM, Graiss G, Kenawy MA (1997) Phys Stat Sol (a) 161:65
34. Abd El-Salam F, Abdel-Khalekh AM, Nada RH, Fawzy A (2008) Mater Charact 59:9
35. Al-Ganainy GS, Mostafa MT, Nagy MR (1998) Phys Stat Sol (a) 65:185
36. Abd El-Salam F, Abdel-Khalekh AM, Nada RH (2000) Eur Phys J Appl Phys 12:159
37. Abd El-Salam F, Abdel-Khalekh AM, Nada RH (2007) Phys Stat Sol (a) 388:217
38. Lui S, Wang B, Tang C, Quians W, Tien F (1995) Mater Sci Forum 175:443